NASA-TM-111805

PERFORMANCE IMPROVEMENT THROUGH INDEXING OF TURBINE AIRFOILS PART 2 - NUMERICAL SIMULATION

Lisa W. Griffin
Computational Fluid Dynamics
National Aeronautics and Space Administration
George C. Marshall Space Flight Center
Marshall Space Flight Center, AL

Frank W. Huber and Om P. Sharma
Technical
Pratt and Whitney
West Palm Beach, FL and East Hartford, CT

ABSTRACT

An experimental/analytical study has been conducted to determine the performance improvements achievable by circumferentially indexing succeeding rows of turbine stator airfoils. A series of tests was conducted to experimentally investigate stator wake clocking effects on the performance of the space shuttle main engine (SSME) alternate turbopump development (ATD) fuel turbine test article (TTA). The results from this study indicate that significant increases in stage efficiency can be attained through application of this airfoil clocking concept. Details of the experiment and its results are documented in part 1 of this paper. In order to gain insight into the mechanisms of the performance improvement, extensive computational fluid dynamics (CFD) simulations were executed. The subject of the present paper is the initial results from the CFD investigation of the configurations and conditions detailed in part 1 of the paper.

To characterize the aerodynamic environments in the experimental test series, two-dimensional (2D), time-accurate, multistage, viscous analyses were performed at the TTA midspan. Computational analyses for five different circumferential positions of the first stage stator have been completed. Details of the computational procedure and the results are presented. The analytical results verify the experimentally demonstrated performance improvement and are compared with data whenever possible. Predictions of time-averaged turbine efficiencies as well as gas conditions throughout the flow field are presented. An initial understanding of the turbine performance improvement mechanism based on the results from this investigation is described.

NOMENCLATURE

AR	Aspect Ratio
C_p	Coefficient of Pressure
c	Axial Chord
P	Pressure
Re	Reynolds Number
s	Entropy
T	Temperature
u	Velocity Magnitude
x	Axial Distance
y^+	Boundary Layer Parameter
Δ	Change in a Quantity
γ	Ratio of Specific Heats
η	Efficiency

Subscripts

ca	Circumferentially-Averaged Quantity
e	Exit Condition
l	Local Condition
me	Turbine Exit Measurement Plane
o	Inlet Condition
s	Static Quantity
t	Total (Stagnation) Quantity
ta	Time-Averaged Quantity
t-t	Total-to-Total Quantity
u	Unsteady Quantity

INTRODUCTION

The objective of the ATD program is to provide line replaceable turbopumps for the SSME. These turbopumps are to be more durable than the baseline SSME turbopumps, but should not change the engine balance. A series of aerodynamic rig tests was conducted by Gaddis et al. (1992) to measure the performance of the ATD high pressure fuel turbopump (HPFTP) turbine. The results would then be compared to the results of the baseline HPFTP turbine tests conducted by Hudson et al. (1991). During the analysis of the data, an interesting phenomenon was uncovered. Turbine

efficiency contours generated from a circumferential mapping of the turbine exit showed not only a 54 cycle pattern corresponding to the second stage vane count, but also a two cycle secondary pattern of +/- 0.5 percentage points. A CFD analysis was conducted to determine the circumferential position of the first vane wake as it approaches the second vane leading edge. These predictions were compared with the measured efficiency contours. This comparison showed that the higher efficiency was measured at the circumferential locations where the first stage vane wakes were predicted to be in general alignment with the leading edges of second stage vanes. It was therefore theorized that turbine performance benefits are attainable by properly aligning the first stage vane wakes relative to the downstream vanes.

In order to test this theory, an experimental/analytical study was conducted. The ATD HPFTP TTA hardware was modified to allow the investigation of the effects of circumferentially indexing succeeding rows of stator airfoils. The experiment, documented in part 1 of this paper (Huber et al., 1994), demonstrated the potential performance benefits. The turbine exit flow field was measured in detail for six first vane clocking positions. These clocking positions were spaced 0.02327 rad (1.333°) apart for a total of 0.11635 rad (6.667°), or one vane pitch as shown in Figure 1. A plot of midspan efficiency versus clocking position (Figure 2) shows a sinusoidal distribution with a delta of 0.8 percentage points.

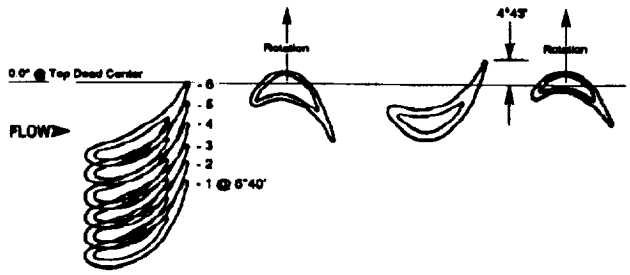

FIGURE 1. FIRST VANE CLOCKING POSITIONS IN RIG

Although the tests demonstrated the vane clocking concept and the resulting potential benefits, the reasons the benefits were achieved were unknown. In order to gain insight into the mechanisms of the performance improvement, extensive CFD analyses were performed. The analytical approach and results are the subjects of this paper. The analytical approach taken was to apply a 2D, time-accurate, multistage, viscous code to the turbine midspan for each of the clocked vane configurations. Results from these CFD investigations include time- and circumferentially-averaged efficiencies, as well as gas conditions throughout the turbine. An initial understanding of the turbine performance improvement mechanism based on the results of this investigation is offered.

TURBINE DESCRIPTION

The clocking concept was tested in a modified version of

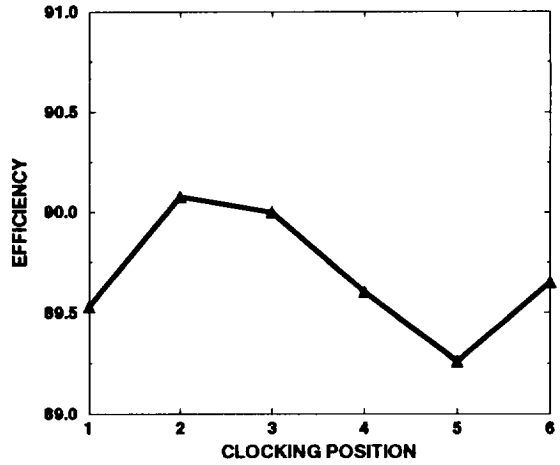

FIGURE 2. EXPERIMENTALLY OBSERVED EFFICIENCY VERSUS CLOCKING POSITION

the ATD HPFTP TTA described by Gaddis et al. (1992). The TTA is a full scale model of the SSME ATD HPFTP turbine. The inlet dome/strut assembly, stators, and rotors accurately duplicate the ATD HPFTP turbine. In order to evaluate the clocking concept, the number of first vanes of the TTA was increased from 52 to 54 to equal the number of second stage vanes. The first stage vanes were then restaggered slightly open to maintain the nominal first vane flow area. The modified turbine consists of two stages with an average diameter of 32.60 cm (12.84 in) and a vane/blade count of 54:50:54:50. The average axial chord is 2.01 cm (0.79 in) and the average axial gap is 1.05 cm (0.41 in). Test conditions corresponding to the calculations presented in this paper involve air entering the first vane at approximately 42.89 m/s (140.71 ft/s) and a Mach number of 0.1226. The total pressure (P_{to}) and the total temperature (T_{to}) at the inlet are 687,000 nt/m^2 (99.6 lbf/in^2) and 982.8K (546 R) respectively. The total-to-static pressure ratio is 1.489, and the Reynolds number (Re) based on axial chord and inlet conditions is 363,500. The rotational speed is 12.19 rad/s (6982 rpm). Additional details on the TTA modifications and the flow conditions for this test series are given in Huber et al. (1994).

METHOD OF SOLUTION

The flow fields for the test series previously described were numerically analyzed using a 2D, time-accurate, viscous code. The methodology, approach, and grid system are discussed in the following sections.

Code Description

The CFD code implemented in this study was STAGE2. STAGE2 predicts the flow through a multistage axial turbomachine with arbitrary blade counts (multiblade) by solving the 2D, unsteady, compressible, thin-layer Navier-

Stokes equations. The code is an extension of an algorithm detailed in Rai and Chakravarthy (1988), Rai (1987), and Rai and Madavan (1988). The code features a time-marching, implicit, third-order spatially accurate, upwind finite difference scheme. The flow field is divided into two types of zones. The inner zones are regions near the airfoil where viscous effects are strong. The thin-layer Navier-Stokes equations are solved in these zones. Euler equations are solved in the outer zones where viscous effects are assumed to be weak. This assumption breaks down in the regions of the outer zones between the airfoils where the wakes pass. However, due to the relative coarseness of the outer grids, the numerical dissipation in the outer regions would be much larger than the viscous effects even if the fully viscous Navier-Stokes equations were solved in these zones. Gundy-Burlet (1990) showed excellent agreement with data when calculating wake profiles when the Euler equations were solved in the outer zones and a fine grid system was employed. Rangwalla et al. (1992) also showed excellent agreement with data when calculating total pressure loss. Boundary conditions enforced at the airfoil surfaces are no slip, adiabatic wall, and a zero normal pressure gradient. At the inlet, the flow angle, upstream Riemann invariant, and average P_{to} are specified while the downstream Riemann invariant is extrapolated from the interior. At the exit, the average static pressure (P_{se}) is specified, while the upsteam Riemann invariant, tangential velocity, and entropy (s) are extrapolated from the interior. The flow is assumed to be fully turbulent. The kinematic viscosity is calculated using Sutherland's law, and the eddy viscocity is estimated using the Baldwin-Lomax turbulence model (Baldwin and Lomax, 1978) implemented in each airfoil's frame of reference. Further details of the STAGE2 code are given in Gundy-Burlet et al. (1989, 1990).

Code Application

The modified SSME ATD TTA has a vane to blade ratio of 54:50:54:50. For this numerical study, the turbine was modeled as having a 1:1:1:1 ratio. The vanes were scaled by 54/50 to provide the correct blockage. For the test series, the first vane clocking positions were spaced at 0.02327 rad (1.333°) apart for a total of 0.11635 rad (6.667°), or one vane pitch. The delta between clocking positions could also be viewed as 20 percent of the vane pitch. Each of these positions provided for a unique flow field. For the analytical investigation, the delta between each clocking position was 20 percent of the scaled vane pitch (Figure 3). Because of the modeled 1:1:1:1 ratio, the scaled vane pitch is 0.12566 rad (7.20°), and the delta between clocking positions is 0.02513 rad (1.44°). In addition, because the turbine is modeled with an equal number of vanes and blades, positions 1 and 6 provide an identical flow field.

The 16 inlet struts that were included in the experiment were not modeled. Previous analysis of the ATD HPFTP turbine by Griffin and Rowey (1993) showed that the strut wake persists through the first stage vane and impacts the first stage blade. Its effect on the second stage is unknown. To model the turbine flow path more accurately, the strut and the interaction of its wake with the first stator wake should be modeled. However, with the addition of the struts, the

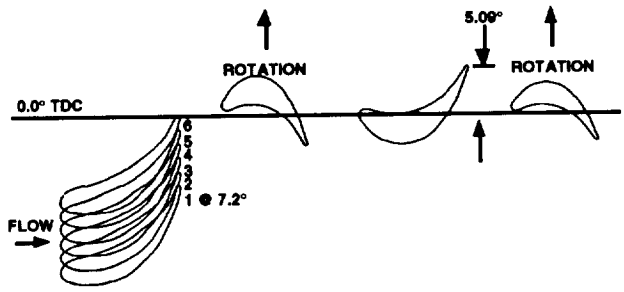

FIGURE 3. NUMERICALLY MODELED FIRST VANE CLOCKING POSITIONS

strut to vane to blade ratio would be approximately 1:3:3:3:3. This larger model would have precluded the analysis of all five test cases due to time and computer memory constraints. The authors believe that the clocking concept can be demonstrated and at least an initial understanding of the mechanism of perrformance enhancement could be determined without including the inlet struts in this analysis.

Calculations were run on the NASA/MSFC CRAY Y-MP. The grid system density and distribution, boundary conditions, initial conditions, and convergence criteria were consistent from case to case. The ultimate convergence criterion was established to be when the time- and circumferentially-averaged, total-to-total efficiency ($\eta_{t\text{-}t}$) stabilized for four significant digits.

Grid System

The grid around each airfoil consists of an inner zone and an outer zone. The inner zone is discretized with a fine 'O' grid surrounding the airfoil. The 'O' grids are overlaid onto 'H' grids which discretize the outer zones. The 'H' grids are patched between blade rows and the rotor 'H' grids slide past stator 'H' grids in time. Each airfoil 'O' grid contains 201 X 51 points with an average y^+ value of 0.8, and each airfoil 'H' grid contains 97 X 79 points. Inflow and outflow grids with 36 X 79 and 39 X 79 points respectively complete the system. The inflow and outflow grids extended approximately 15 chord lengths upstream and downstream of the turbine respectively. The axial spacing increased with distance from the turbine to damp the amplitudes of propagating wave modes as prescribed by Rangwalla and Rai (1993). The total number of points in the grid system (shown in Figure 4) is 77,581.

Grid densities for this study are finer than those used by Rangwalla et al. (1992) who showed excellent agreement with data when calculating midspan total pressure loss for a 1 1/2 stage turbine. The grid dimensions in that study were 151 X 41 and 90 X 71 for the inner and outer grids respectively. The *Re* per inch based on inlet conditions was 100,000 and the blade pitch was 15.39 cm (6.06 in). In the current study, the *Re* per inch is 460,000 so the airfoil wakes should be slightly thinner which would necessitate a finer grid in the circumferential direction. However, the blade pitch in this study is 1.48 cm (0.583 in) or 9.6% of the blade pitch of the turbine analyzed by Rangwalla et al. Therefore, the authors

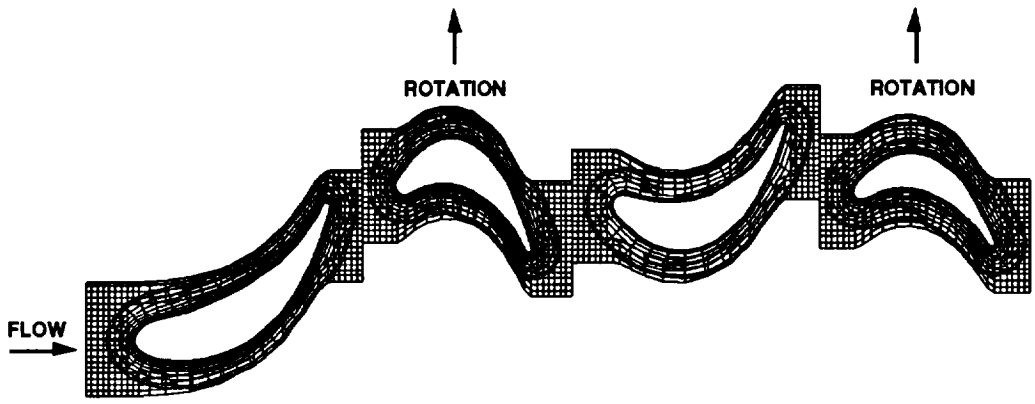

FIGURE 4. MODIFIED ATD FUEL TURBINE GRID (EVERY 4TH POINT IN EACH DIRECTION SHOWN; INFLOW AND OUTFLOW GRIDS NOT SHOWN

believe that the grids used in this study were adequate to meet the objectives of the analysis.

RESULTS AND DISCUSSION

Total-to-total efficiency was used to quantify the effect of the vane clocking on turbine performance. The η_{t-t} was calculated by Equation 1

$$\eta_{t-t} = \frac{T_{to,ca,ta} - T_{tme,ca,ta}}{T_{to,ca,ta}\left[1.0 - \left(\frac{P_{tme,ca,ta}}{P_{to,ca,ta}}\right)^{\frac{\gamma-1}{\gamma}}\right]} \quad (1)$$

where *ta* denotes a time-averaged quantity, *ca* indicates a quantity spatially averaged in the circumferential direction, *o* is the computational inlet, and *me* is the plane which represents the location where the efficiency was measured in the test series. The quantities were time-averaged over 1000 time slices which comprised one periodic rotor passage. The predicted turbine midspan efficiencies are given in Table 1.

POSITION	EFFICIENCY
1	94.82%
2	94.95%
3	94.87%
4	94.74%
5	94.65%
6	94.82%

TABLE 1. PREDICTED TOTAL-TO -TOTAL EfFFICIENCY - 2 STAGE CONFIGURATION

A prediction of η_{t-t} at the turbine midspan is shown in Figure 5. Both the data and prediction show a sinusoidal pattern of η_{t-t} versus clocking position. However, the data shows an average efficiency of 89.7% with a $\Delta\eta_{t-t}$ of +/-0.4% while the prediction shows an average efficiency of 94.80% +/- 0.15%. The difference in the average level of η_{t-t} can be explained by the types of losses that are generated by the two techniques. For the experiment, the losses are not truly midspan losses. Because this turbine has small blades with a low aspect ratio (AR=1.3), the endwalls provide some spanwise mixing. The calculation provides strictly midspan profile loss. A meanline analysis of the turbine with all losses but profile losses deleted predicted a midspan efficiency of 94.90%. There could be several reasons for the difference between the observed and predicted $\Delta\eta_{t-t}$. The first vane clocking could reduce the endwall losses in the downstream vane or blade row. This effect would not modeled in a 2D calculation. It is also possible that the difference is due to a limitation in the analytical technique due to numerical error. In any event, the difference can not be explained at this time, and further work is needed.

In order to isolate whether the performance improvement was due to changes in the flow field of the second vane or the second blade, η_{t-t} was calculated for 1 1/2 stages. The predicted 1 1/2 stage efficiencies are shown in Table 2 and plotted in Figure 6. The sinusoidal pattern is still evident, and the $\Delta\eta_{t-t}$ is + /- 0.14%. This result indicates that improved second vane performance is a major contributor to the efficiency gain obtained by vane clocking. Therefore, the remainder of the paper will concentrate on performance improvements in the second vane.

POSITION	EFFICIENCY
1	92.21%
2	92.36%
3	92.26%
4	92.08%
5	92.12%
6	92.21%

TABLE 2. PREDICTED TOTAL-TO -TOTAL EFFICIENCY -

1 1/2 STAGE CONFIGURATION

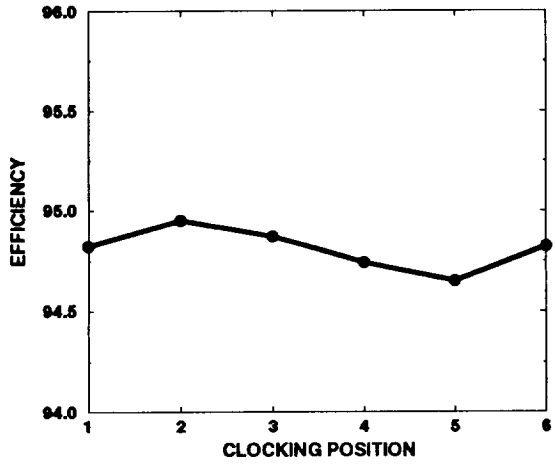

FIGURE 5. PREDICTED 2 STAGE EFFICIENCY VERSUS CLOCKING POSITION

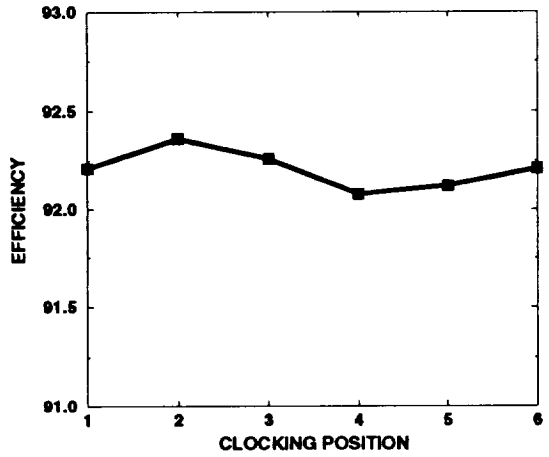

FIGURE 6. PREDICTED 1 1/2 STAGE EFFICIENCY VERSUS CLOCKING POSITION

Entropy contours were generated in order to visualize the airfoil wakes. The first vane wake is chopped into discrete pulses by the passing first blade. These pulses leave the rotor at fixed circumferential locations relative to the second vane. When the flow field is time-averaged, the pulses appear as a continuous streak into the second vane. Figures 7a and b show time-averaged entropy contours (s_{ta}) for the second vane for positions 2 and 5. These vane clocking positions were predicted and measured to produce the highest and lowest turbine efficiencies respectively. In Figure 7a, it is shown that the first vane wake represented by s_{ta} contours impinges upon the leading edge of the second vane when the first vane is clocked to position 2. Figure 7b shows that when the first vane is clocked to position 5, its wake passes through the mid-channel of the second vane. These results confirm the earlier CFD predictions for wake positions in the baseline SSME ATD HPFTP turbine.

One possible reason for the increased performance of the second vane is reduced surface velocities. When the first and second stage vanes are clocked so that the time-averaged first vane wake is aligned with the leading edge of the second vane (as in position 2), the second vane has lower surface velocities. Figure 8 shows time-averaged pressure coefficients for the second vane defined in Equation 2

$$C_p = \frac{P_{sl}}{P_{T,airfoil}} \qquad (2)$$

for positions 2 and 5. The plot indicates higher surface velocities for the second vane when the first vane is clocked to position 5. In fact, the average surface Mach numbers for the second vane for positions 2 and 5 are 0.437 and 0.471 respectively. Assuming that the dissipation coefficients are constant, the loss can be estimated to be proportional to the difference in the u^3 (Denton, 1993). This estimate indicates that the reduced losses due to lower velocities accounts for 73% of the efficiency difference or $\Delta\eta_{t\text{-}t} = 0.22$.

Another possible reason for increased second vane performance is reduced flow unsteadiness when the vanes are optimally indexed. An increase in unsteadiness would generate additional losses due to increased turbulence. Animation of the unsteady entropy contours shows that the first vane wake is chopped into discrete pulses by the first blade. When the vanes are optimally indexed, these higher entropy regions from the first vane fill in between first rotor wakes at the second vane leading edge. This phenomenon can be seen in Figure 9 which shows instantaneous entropy contours for the second vane at four different times within a blade passage for clocking positions 2 and 5. The black areas indicate relatively lower regions of loss. Comparison of Figures 9a and b show that when the vanes are optimally indexed (as in position 2) the second vane leading edge is always in a region of higher loss made up of the chopped first vane wakes along with first blade wakes. When the first vanes are in position 5, their chopped wakes travel midway between second vanes. This results in a more discrete first blade wake passing the second vane leading edge, thus increasing the local variation in entropy. Figures 10 a and b show unsteady C_p at points near the leading edge of the second vane on the pressure surface and suction surface respectively versus blade passage. To aid visualization, the plot is repeated for four blade passages. The increase in the flow field unsteadiness of the position 5 case over the position 2 case is illustrated. On the pressure side, the standard deviation from the time-average is calculated to be 0.00597 for position 2 and 0.00667 for position 5 demonstrating an increase of 11.8% in unsteadiness for position 5 over position 2. On the suction side, the standard deviation from the time-average was 0.00590 for position 2 and 0.00745 for position 5 showing an increase of 26% in unsteadiness for position 5 over position 2.

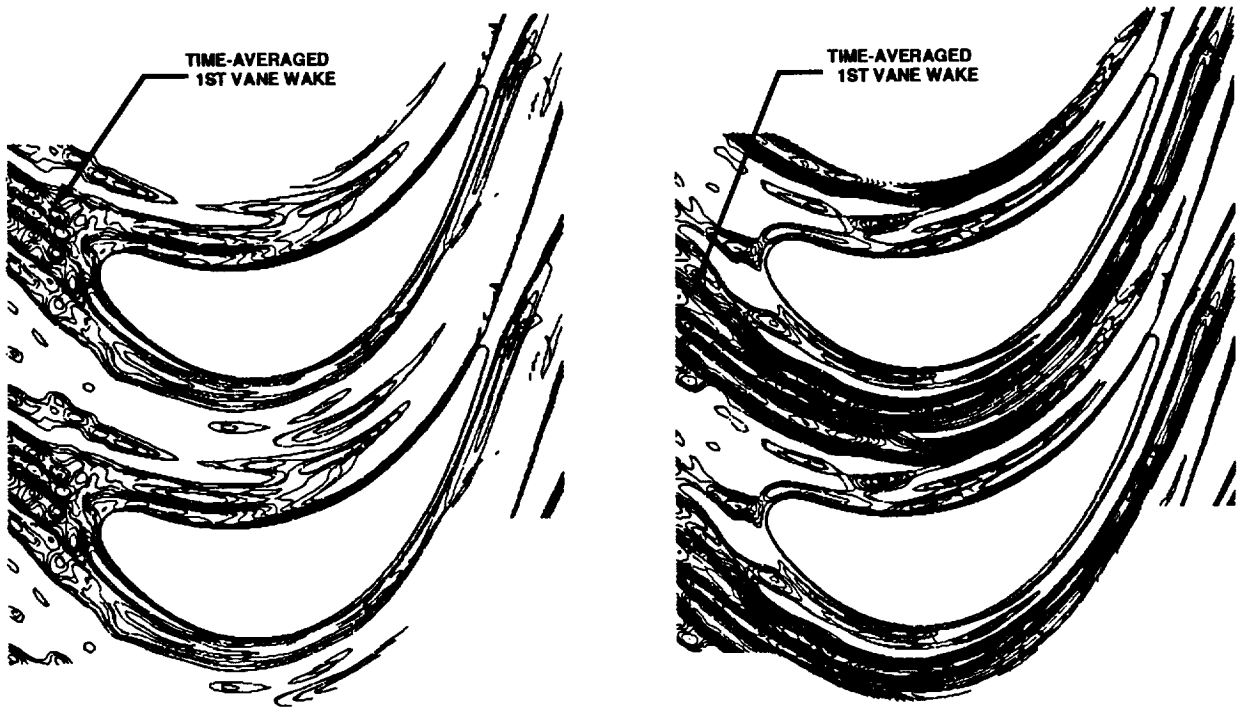

FIGURE 7. TIME-AVERAGED ENTROPY CONTOURS FOR THE SECOND VANE WITH THE FIRST VANE CLOCKED TO (a) POSITION 2 AND (b) POSITION 5

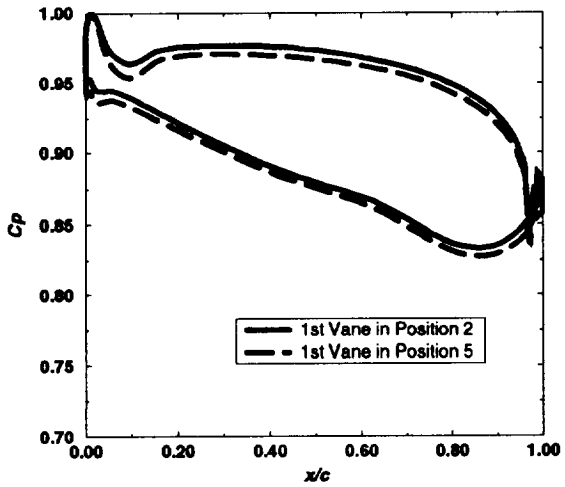

FIGURE 8. PRESSURE COEFFICIENTS FOR THE SECOND VANE

CONCLUSIONS

Two-dimensional, time-accurate, Navier-Stokes simulations of the vane indexing experiment have been performed. The primary objective of the investigation was to provide insights into the mechanisms of the turbine performance improvement observed in the experiment. The analysis has provided a vast amount of information that is essential to achieving the objective. Although the results have not been fully interrogated at this time, several candidate mechanisms have been identified.

The numerical analysis correctly predicts the indexing positions of the first and second stage vanes required to produce maximum efficiency. The sinusoidal pattern of turbine midspan efficiency versus clocking position that wasseen in the data was also predicted. However, the magnitude of the predicted $\Delta\eta_{t\text{-}t}$ is less than experimentally observed. The most probable reason for the difference is the 2D nature of the analysis, although limitations in numerical accuracy are possible.

The computational results indicate that improved performance of the second vane is a major contributor to the turbine efficiency benefits achievable through vane indexing. Best performance is predicted to be obtained when the time-averaged first vane wake is aligned with the second vane leading edge . Reduced surface velocities and less large-scale unsteadiness on the second vane are seen as possible reasons for the improved second vane performance.

The results from this numerical investigation show that the turbine airfoil indexing phenomenon is predictable and illustrates how to achieve this phenomenon in the hardware. Questions remain as to the exact mechanisms involved.

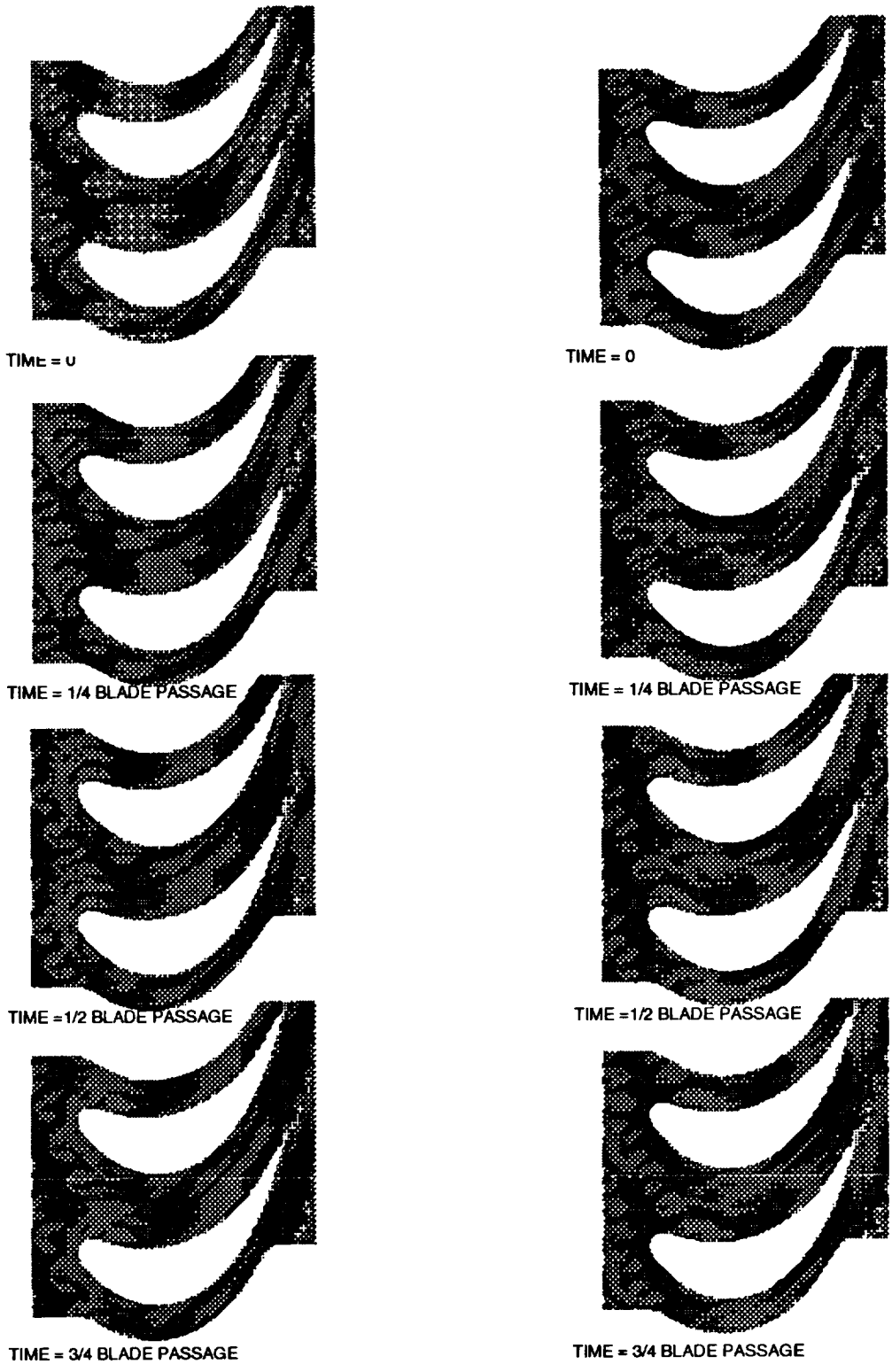

(a) (b)

FIGURE 9. INSTANEOUS ENTROPY CONTOURS AT FOUR TIME SLICES FOR THE SECOND VANE WITH THE FIRST VANE CLOCKED TO (a) POSITION 2 AND (b) POSITION 5

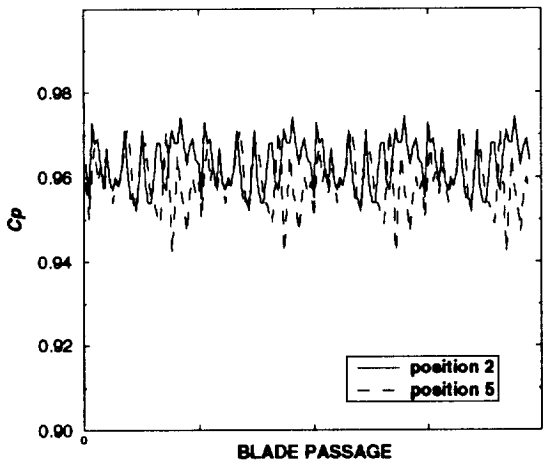

(a)

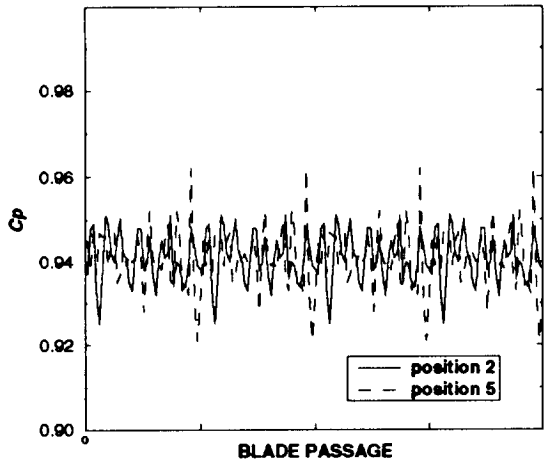

(b)

FIGURE 10. UNSTEADY PRESSURE COEFFICIENTS AT THE LEADING EDGE OF THE SECOND VANE

Further interrogation of the existing results may identify additional candidate mechanisms and provide guidance for further analysis. Three-dimensional analysis will also be necessary for the best and worst clocking positions to investigate possible effects of the vane clocking on endwall losses.

ACKNOWLEDGMENTS

The authors wish to acknowledge the important contributions made to this work by our colleagues. A. J. Fredmonski and Dean Johnson of Pratt and Whitney performed supporting analyses for this work. Karen Gundy-Burlet of NASA/Ames Research Center resolved issues pertaining to STAGE2. We are very appreciative of their support. We are also thankful for the graphics work performed by Catherine Dumas formerly Sverdrup Technology and Denise Doran of NASA/MSFC and for the support for the NASA/MSFC personnel provided by the Office of Advanced Concepts and Technology.

REFERENCES

Denton, J.D., 1993,"Loss Mechanisms in Turbomachines," Journal of Turbomachinery, Vol. 115, pp. 621-658.

Gaddis, S. W., Hudson, S. T., and Johnson, P. D., 1992, "Cold Flow Testing of the Space Shuttle Main Engine Alternate Turbopump Development High Pressure Fuel Turbine Model," ASME Paper No. 92-GT-280.

Griffin, L. W., and Rowey, R. J., 1993, "Analytical Investigation of the Unsteady Aerodynamic Environments in Space Shuttle Main Engine (SSME) Turbines," ASME Paper No. 93-GT-362.

Gundy-Burlet, K. L., Rai, M. M., and Dring, R. P., 1989, "Two-Dimensional Computations of Multi-Stage Compressor Flows using a Zonal Approach," AIAA Paper No. 89-2452.

Gundy-Burlet, K. L., Rai, M. M., Stauter, R. C., and Dring, R. P., 1990, "Temporally and Spatially Resolved Flow in a Two-Stage Axial Compressor, Part II-Computational Assessment," ASME Paper No. 90-GT-299.

Huber, F. W., Johnson, P. D., Sharma, O. P., Staubach, J. B., and Gaddis, S. W., 1994, "Performance Improvement Through Indexing of Turbine Airfoils, Part 1 - Experimental Investigation," to be presented at the 1995 ASME IGTI Conference.

Hudson, S. T., Gaddis, S. W., and Johnson, P. D., 1991 "Cold Flow Testing of the Space Shuttle Main Engine High Pressure Fuel Turbopump Turbine Model," AIAA Paper No. 91-2503.

Rai, M. M., and Chakravarthy, S. R., 1986, "An Implicit Form for the Osher Upwind Scheme," AIAA Journal, Vol. 24, No. 5 pp. 735-743.

Rai, M. M., 1987, "Unsteady Three-Dimensional Navier-Stokes Simulations of Turbine Rotor-Stator Interaction," AIAA Paper No. 87-2058.

Rai, M. M., and Madavan, N. K., 1988, "Multi-Airfoil Navier-Stokes Simulations of Turbine Rotor-Stator Interaction," AIAA Paper No. 88-0361.

Rangwalla, A. A., Madavan, N. K., and Johnson, P. D., 1992, "Application of an Unsteady Navier-Stokes Solver to Transonic Turbine Design," Journal of Propulsion and Power, Vol. 8, No. 5, pp. 1079-1086.

Rangwalla, A. A, and Rai, M. M., 1993, "A Numerical Analysis of Tonal Acoustics in Rotor-Stator Interaction," Journal of Fluids and Structures, Vol. 7, pp. 611-637.